The generation of mode-1 and mode-2 nonlinear internal waves on the upstream side of a large sill of the Mascarene Ridge (Indian Ocean).

J.C.B. da Silva (1), M. Buijsman (2) and J.M. Magalhaes (1)

(1) CIIMAR – Interdisciplinary Centre of Marine and Environmental Research & Department of Geosciences, Environment and Spatial Planning, University of Porto, Rua dos Bragas 289, 4050-123 Porto, Portugal.

(2) Department of Physics, University of New Orleans, 2000 Lakeshore Dr., New Orleans, LA 70148, USA.

REFERENCES:

Buijsman, M.C., Kanarska, Y., McWilliams, J.C., 2010. On the generation and evolution of nonlinear internal waves in the South China Sea. J. Geophys. Res. 115, C02012.

da Silva, J.C.B., New, A.L., Magalhaes, J.M., 2011. On the structure and propagation of internal solitary waves generated at the Mascarene Plateau in the Indian Ocean. Deep-Sea Res. I 58, 229-240.

Guo, C., Vlasenko, V., Alpers, W., Stashchuk, N., Chen, X., 2012. Evidence of short internal waves trailing strong internal solitary waves in the northern South China Sea from synthetic aperture radar observations. Remote Sensing of Environment 124, 542–550.

New, A.L., Magalhaes, J.M., da Silva, J.C.B., 2013. Internal solitary waves on the Saya de Malha bank of the Mascarene Plateau: SAR observations and interpretation. Deep-Sea Res. I 79, 50–61.

Vlasenko, V., Stashchuk, N., Guo, C., Chen, X., 2010. Multimodal structure of baroclinic tides in the South China Sea. Nonlinear Processes in Geophysics 17, 529–543.

INTRODUCTION:

Strong tidal flow over a sill generates Internal Solitary Waves (ISWs) close to the area of topographic interaction. This may occur either upstream or downstream of the sill, being respectively explained by two different mechanisms: "internal tide release" or "lee wave generation". We aim to clarify the generation process at work to the east of the Mascarene Plateau (Indian Ocean) using Synthetic Aperture Radar (SAR) imagery and MITgcm nonhydrostatic simulations. Realistic representations of stratification and bathymetry are used with asymmetric tidal forcing (including the steady South Equatorial Current) along a 2D vertical section, which is identified as an effective nonlinear internal wave generator from the SAR. Two different types of nonlinear wave trains and generation mechanisms associated with westward barotropic flow over the sill are observed in the SAR data and simulated with the model. The first generation mechanism is a process involving an elevation wave (due to blocking and upstream influence) with a higher energy density east of the ridge, which is released eastwards as soon as the tidal current slackens. On its backslope strong mode-1 solitons develop upstream of the sill. The (steady + tidal) flow is subcritical with respect to first-mode internal waves, but supercritical with respect to higher wave modes. A massive mode-2 lee wave is generated downstream of the sill, which is trapped there during maximum westward tidal flow and released upstream when the tide relaxes. However, this large lee wave does not evolve into a train of (mode-1) solitary waves as it propagates westward. The underwater sill being investigated is in the mixed tidal lee wave regime, where the internal tide release mechanism, lee wave generation and internal wave beams can coexist. Furthermore, large eastward propagating interfacial mode-2 nonlinear internal waves are observed for a long distance (and time) upstream of the sill. A second generation mechanism for those mode-2 interfacial nonlinear internal waves is then investigated, which is consistent with beam scattering into the pycnocline by an internal wave beam that originates from critical topography on the leeward (i.e. westward) side of the sill (**see Figure 1**). This new generation mechanism may be at work in many other regions of the ocean, but not yet realized. See **Figure 2** for locations.

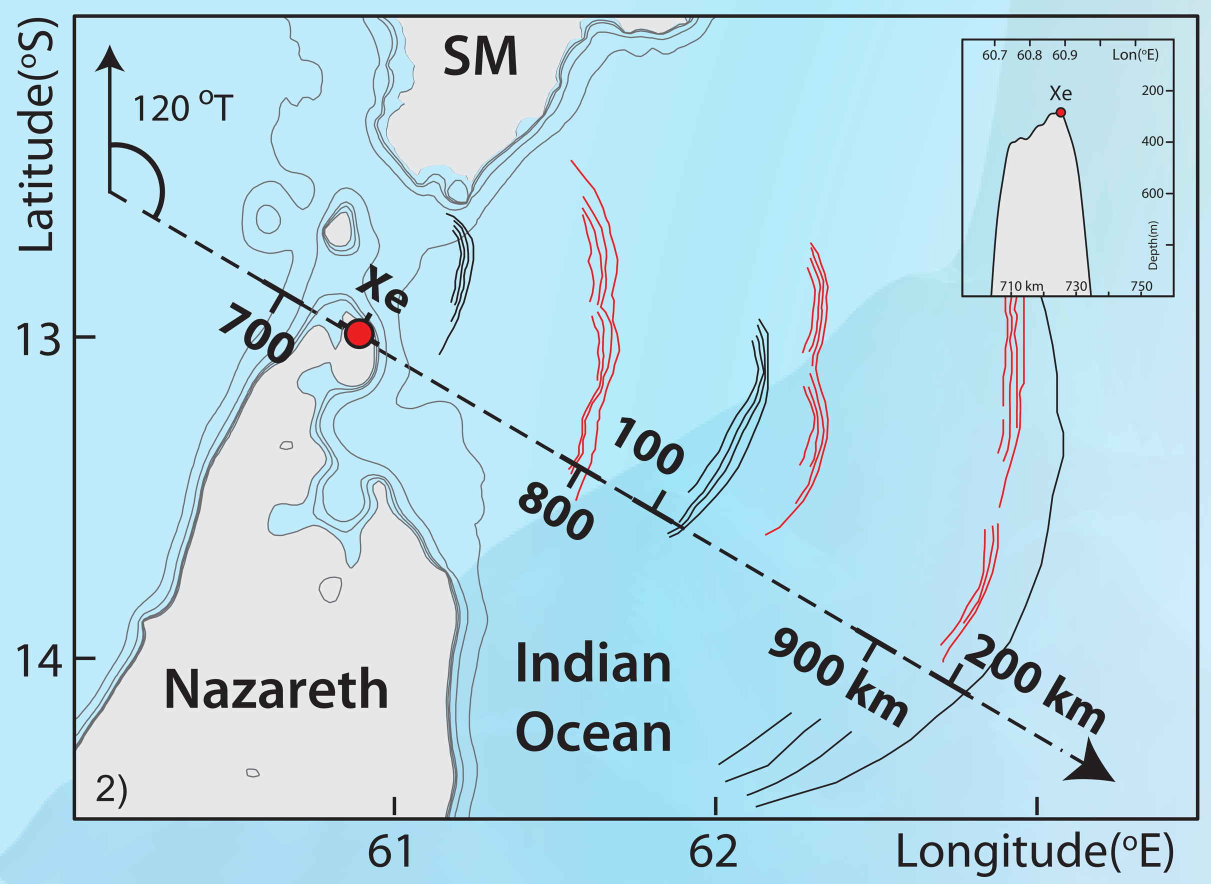

Figure 3 shows the combined results of model and SAR data. The red (filled) dots and the red linear fit to those dots represent the SAR data, while the open green circles refer to the model results and show the space versus time evolution of the leading (mode-1) soliton in a wave packet. SAR and model data are aligned with each other. The best (linear) fit through the SAR data (red line in **Figure 3**) intersects the origin of a frame of reference centred at position Xe (60.8917 °E, 12.9792 °S; see **Figure 2**) and slack (barotropic) tide (transition from westward to eastward tidal flow). This is the generation coordinate for the mode-1 (primary) solitary wave trains according to the MITgcm. However, according to the satellite data another possibility would be 12.6 km upstream of position Xw (see **Figure 3**), on the lee side of the sill at the time of maximum westward flow, as originally proposed in **da Silva et al. (2011)** and **New et al. (2013)**. Two other curves correspond to the trajectory predicted by linear theory (Taylor-Goldstein equation) for long IWs generated at Xe (crest on the upstream side of the sill) at the time of slack tide (dark continuous curve in **Figure 3**), and the trajectory of long IWs generated at Xw at the time of maximum westward (barotropic) tidal flow (grey curve in **Figure 3**). As expected from nonlinear theory, the slopes of the fits to the data (model and SAR) are slightly steeper than those predicted from linear theory. This means that the nonlinear wave speeds of the ISWs are slightly higher than linear theory predicts. In addition, the grey (linear) trajectory with origin at Xw at the time of maximum westward flow is significantly offset from the data points (both model and SAR). This supports that these ISWs are generated very closely to position Xe at the time of slack tide (transition from westward to eastward flow), since the fit crosses the origin at this coordinate.

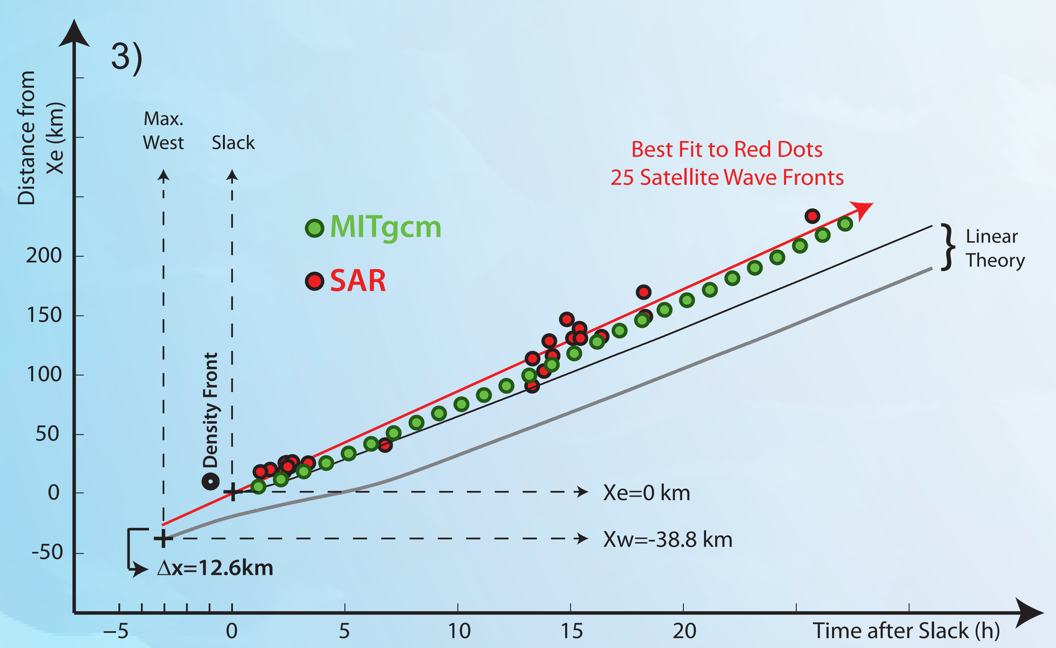

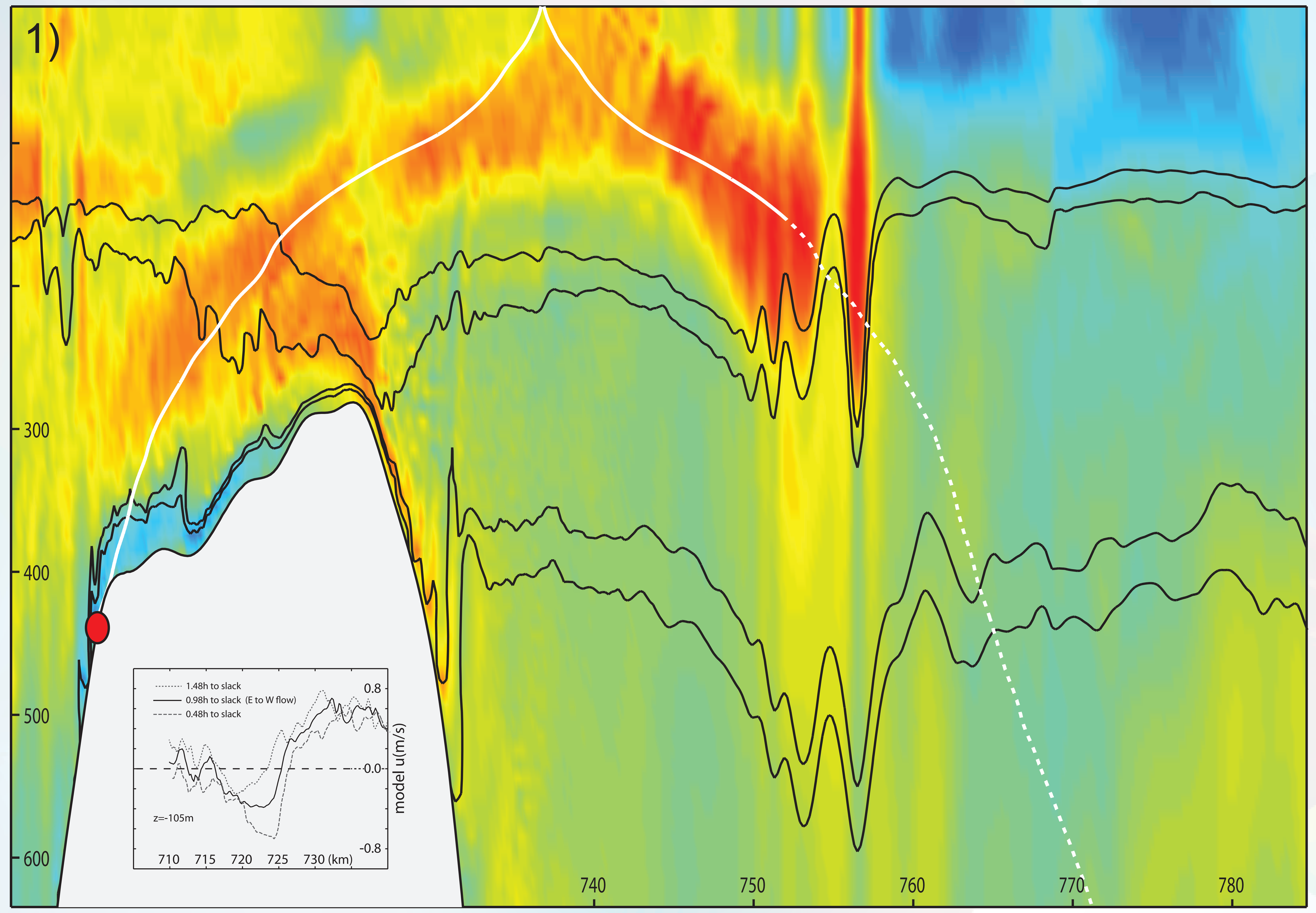

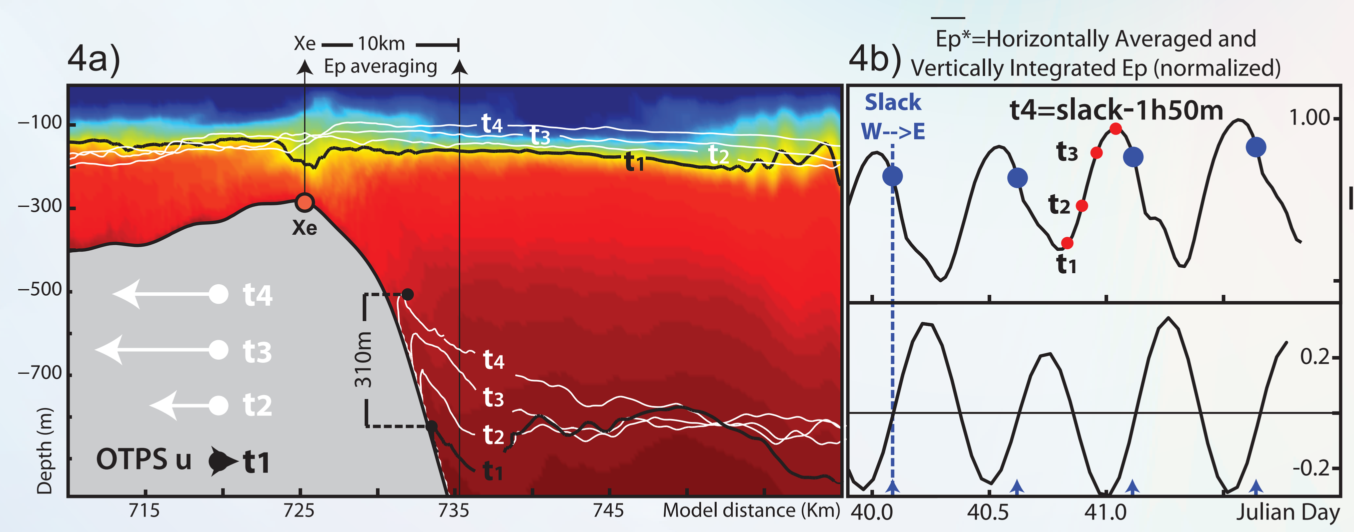

The upstream character of the model response is evident in **Figure 4a**, which shows the displacement of some given isopycnal at depths significantly greater than the sill's crest (around 800 m), at 1.5 hour intervals (from time t1 to t3) and then after 1 hour and 50 minutes (at time t4) (see deeper isopycnals in **Figure 4a**). At the time of slack tide (tide transition from east to westward flow), the far upstream depth of this isopycnal (black line) lies beneath 800 m on average. According to the evolution seen in **Figure 4a**, this isopycnal is displaced upward against the topography, but never makes it over the crest and the flow at those depths is totally blocked. A long wave is launched upstream, which gently raises isopycnals in the upper layer (near the base of the mixed layer), leading to a shoaling of the pycnocline in the far field (seen in the time evolution of the upper isopycnal in **Figure 4a**, extending some 30 km from the sill's crest in the upstream direction). Behind this elevation wave, the pycnocline initially slopes gently downward, gradually steepens, and forms a mode-1 solitary wave train. All these stages can be seen in the model simulation. A time series for the available potential energy is computed (see **Buijsman et al., 2010**) along four consecutive (semi-diurnal) tidal cycles (see **Figure 4b**). For each time frame was vertically integrated and averaged along a 10 km horizontal section as indicated in **Figure 4a** (which after normalization is shown in **Figure 4b**). This energy density averaging is representative of the domain upstream of Xe, i.e. the ISW generation region. This energy analysis clearly accounts for the presence of an elevation wave matching the precise location of the assumed generation location (upstream of Xe) of the mode-1 ISWs.

MODE-2 NONLINEAR INTERNAL WAVES:

We report, for the first time, the existence of long-lived mode-2 nonlinear IWs coupled with wave-tails composed of mode-1 smaller-scale ISWs, in the study region. These coherent features can propagate for distances in excess of 100 km (**Figure 2** and **Figure 5**) to the east side of the sill with typical longevities exceeding a semi-diurnal tidal cycle. The mode-2 IW structures are captured in the SAR mainly due to their associated first mode ISWs (in the same fashion as those reported in **Guo et al., 2012** for the South China Sea). The generation mechanism of these long-lived mode-2 IWs is consistent with beam scattering into the pycnocline by an internal (tidal) beam, also known as "local generation" of solitary waves. They result from the impact of internal (tidal) wave beams with the existing pycnocline some 50 km upstream of the origin of the (primary) mode-1 ISWs. This internal wave beam develops in the MITgcm model soon after slack tide (i.e. transition from west to eastward flow), when multi-modal internal waves are free to propagate upstream (to the east). It originates on the lee (i.e. westward) side of the sill from critical (topographic) slopes, leaning upwards and eastwards and reflecting from the sea surface, after which the beam generates mode-2 solitary-like IWs through a resonant process. These then propagate along the pycnocline for long distances, producing a velocity field with favorable conditions for sustaining their associated wave-tails (in the same manner as reported in **Guo et al., 2012** and **Vlasenko et al., 2010**).

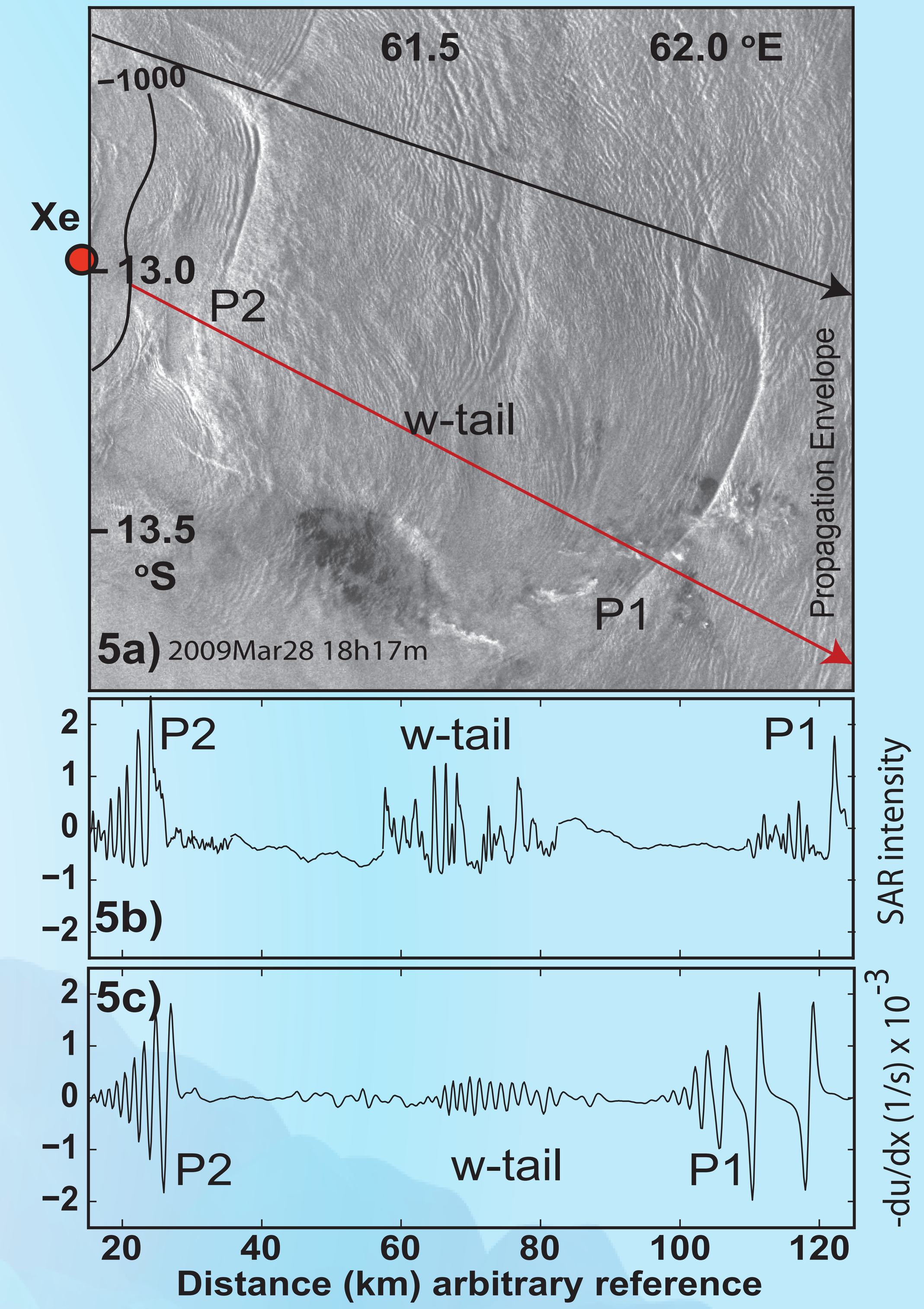

Figure 6 shows model data points (in green) for mode-2 IWs travelling upstream (i.e. eastwards) of the sill as well as the SAR leading signatures (in red) of wave-tails. The data points comprise approximately 30 hours (i.e. more than 2 complete semi-diurnal tidal cycles) and reach to about 150 km away from the sill. The travel-time graph is assembled in the same manner as it has been done for mode-1 IWs (**Figure 3**). Note the model consistency along a linear fit to the SAR data (red line in **Figure 6**). Two additional curves are drawn in this travel-time graph: 1) a propagation trajectory for linear (mode-1) long IWs, with an origin at the sill's crest (Xe=0) by the time of slack tide (i.e., tide reversal from westward into eastward flow) and 2) a similar curve but for mode-2 IWs, whose slope is thus significantly smaller than for mode-1 waves (see dark continuous lines in **Figure 6**). The slope of the data (both model and SAR) in **Figure 6** almost matches that of mode-2 linear waves, being however slightly steeper than this (owing to nonlinear effects). We thus conclude that the "wave tails" propagate with a speed close to (but slightly superior) the mode-2 long linear IWs. This travel-time diagram suggests that the generation of those "long-lived" mode-2 IWs occurs some 45-50 km from Xe (i.e. near the location where the IT beam impacts the thermocline form above, see **Figure 1**), 8 hours after slack tide (i.e. reversal from westward into eastward tidal flow, see also green dashed lines in **Figure 6**). The data thus support the idea of the existence of at least two different types of mode-2 IWs: 1) short-lived IWs whose lifetime is generally approximately 5 hours (around some 10-15 kms from their origin, and displayed as smaller blue filled circles in **Figure 6**), which propagate in the vicinity of the sill, and 2) long-lived waves away from the sill that last for at least 22 hours.